





RESEARCH ARTICLE

MRI- and CT-based metrics for the quantification of arthroscopic bone resections in femoroacetabular impingement syndrome

Martina Guidetti¹  | Philip Malloy^{1,2}  | Thomas D. Alter¹ |
Alexander C. Newhouse¹ | Alejandro A. Espinoza Orías¹  | Nozomu Inoue¹ |
Shane J. Nho¹ 

¹Section of Young Adult Hip Surgery, Division of Sports Medicine, Department of Orthopedic Surgery, Rush Medical College of Rush University, Rush University Medical Center, Chicago, Illinois, USA

²Department of Physical Therapy, Arcadia University, Glenside, Pennsylvania, USA

Correspondence

Martina Guidetti, Department of Orthopedic Surgery, Rush Medical College of Rush University, Rush University Medical Center, 1611 W Harrison St, Chicago, IL 60612, USA.
Email: martina.guidetti@rush.edu

Abstract

The purpose of this in vitro study was to quantify the bone resected from the proximal femur during hip arthroscopy using metrics generated from magnetic resonance imaging (MRI) and computed tomography (CT) reconstructed three-dimensional (3D) bone models. Seven cadaveric hemipelvises underwent both a 1.5 T MRI and CT scan before and following an arthroscopic proximal femoral osteochondroplasty. The images from MRI and CT were segmented to generate 3D proximal femoral surface models. A validated 3D-3D registration method was used to compare surface-to-surface distances between the 3D models before and following surgery. The new metrics of maximum height, mean height, surface area and volume, were computed to quantify bone resected during osteochondroplasty. Stability of the metrics across imaging modalities was established through paired sample t-tests and bivariate correlation. Bivariate correlation analyses indicated strong correlations between all metrics ($r = 0.728$ – 0.878) computed from MRI and CT derived models. There were no differences in the MRI- and CT-based metrics used to quantify bone resected during femoral osteochondroplasty. Preoperative and postoperative MRI and CT derived 3D bone models can be used to quantify bone resected during femoral osteochondroplasty, without significant differences between the imaging modalities.

KEYWORDS

femoroacetabular impingement syndrome, hip arthroscopy magnetic resonance imaging, three-dimensional analysis

1 | INTRODUCTION

Hip preservation surgery often involves arthroscopic or open osteochondroplasty to reshape abnormal bone geometry to restore a congruent articulation at the hip joint for function.^{1,2} In recent years

considerable interest has grown around these surgeries performed to treat painful hip conditions, such as femoroacetabular impingement syndrome (FAIS). In the case of cam-type FAIS, an osteochondroplasty of the proximal femur is designed to recontour the abnormal shapes of the head and neck junction such that a normal offset between the

head and neck transition is restored. This structural remodeling also corrects abnormal mechanics that are known to contribute to the development of idiopathic hip osteoarthritis (OA), and ultimately to the need for a total hip replacement.^{3,4} Currently, for the diagnosis and quantification of cam-type morphology, the field mainly relies on two-dimensional (2D) radiographs. Since abnormal bony morphology clearly constitutes a three-dimensional (3D) problem, the clinical use of radiographs as screening modality still represents a significant barrier for the morphological evaluation, despite new techniques have been proposed to three-dimensionally approach cam-type FAIS resections.^{5–15} The consequence of inadequate 3D morphologic assessment is potential incomplete resection of the proximal femur to address cam-type FAIS, which has been cited as the primary reason for revision surgery.^{16–20} The current clinical approach for the quantification of proximal femur bony morphology also exposes patients to ionizing radiation, in cases of both radiographs and computed tomography (CT).^{21,22}

Magnetic resonance imaging (MRI) is a valid alternative imaging modality to reconstruct osseous 3D models when compared to the clinical gold standard of CT.^{23–28} Although most studies have previously compared 3D bone models derived from CT and 3T MRI,^{21,29–32} advancements in the MRI sequences that are now widely available and commonly used, have made it possible to obtain osseous 3D models with CT-like resolution using 1.5 T MRI scans.³³ It has recently been demonstrated that 1.5 T MRI can generate accurate 3D proximal femoral models with absolute agreement when compared to the clinical gold standard of CT derived models and laser scanner ground truth models of excised femurs.²⁵ Since 1.5 T MRI scanners are widely available in the orthopedic clinical setting, and advancements in the artificial intelligence field are making the segmentation of bone from MRI images an automatic and quicker process, thus easier for widespread clinical use, a shift towards minimizing or eliminating ionizing radiation exposure in the hip preservation setting is warranted.^{34–42} Additionally, the ability of MRI to assess multiple tissues with a single imaging modality, streamlines the preoperative workup by reducing the burden of multiple diagnostic imaging tests for patients. The use of MRI also opens the field for opportunities to generate new metrics to accurately estimate the 3D nature of bony deformities.¹¹

Techniques that merge the surfaces of 3D bone models have been used to compare models generated from different imaging modalities.^{23,25–28} In the present cadaveric study, we sought to compare the surfaces of 3D bone models reconstructed from 1.5 T MRI and CT scans performed before and after hip arthroscopy to quantify bone resected during an arthroscopic femoral osteochondroplasty. As such, the purpose of this invitro study was to quantify the bone resected from the proximal femur during hip arthroscopy using metrics generated from MRI and CT derived 3D models. The metrics were compared across imaging modalities that are currently used clinically to generate 3D bone models for surgical planning. Therefore, the present study could help to unveil new methods for the quantification of cam-type FAIS pathomorphology and advance the diagnosis and treatment of this hip disorder.

2 | MATERIALS AND METHODS

2.1 | Specimen selection

Seven freshfrozen, unpaired human cadaveric hemipelvises were procured through a certified tissue bank as part of another study. All cadavers were screened for metastatic cancer to the bones, communicable diseases before procurement, and prior surgical intervention. Cadavers with an alpha angle greater than 45°, as measured on the axial slice of MRI and CT imaging, were selected. All cadavers were screened for evidence of OA (Tönnis grade >1) using standard radiographs. The average donor age and BMI were 51.0 ± 12.5 years old and 19.3 ± 3.6 kg/m², respectively. All specimens were stored in a laboratory freezer at 20°C until approximately 48 h before use and then thawed to room temperature for testing and imaging.

2.2 | Imaging and image processing

Each intact cadaveric pelvis was thawed to room temperature before undergoing pre and postoperative MRI and CT imaging of the pelvis, from the iliac crest to midfemoral diaphysis.^{43,44} All MRIs were performed on a 1.5 T MAGNETOM Espree system (Siemens Healthcare) using an MRI sequence previously described²⁵ with the following modifications: field of view = 540×288 mm, total scan time = 9 min and 11 s, resulting in 144 axial slices. The previously described sequence has been shown to provide CT-like images from MRI to be used for bone segmentation.³³ CT scans were performed on a GE Brightspeed CT system (GE Healthcare; BrightSpeed) as previously described.²⁵ All MRIs and CTs were exported as Digital Imaging and Communication in Medicine files and stored in an institutional Picture Archiving and Communication System. A semiautomatic segmentation process was performed using commercially available segmentation software (Materialise Mimics, v. 21 Research) to reconstruct the 3D bone models. All segmentations were performed by a trained biomedical engineer (A.C.N). The number of iterations and smooth factor parameters for smoothing the 3D model were set to 2 and 0.5, respectively. The accuracy of the reconstruction process had been previously determined by quantifying the average absolute distance between MRI and laser scanned reconstructed models and between MRI and CT reconstructed models, being less than 0.3 and 0.4 mm, respectively.²⁵ The accuracy for the reconstruction of bone models from MRI had been also quantified in a different study by computing the absolute dimensional errors and it was found that both CT and MRI are accurate for 3D bone reconstructions within 0.5 mm compared to optical scans of the bare (without any soft tissue attached to it) bone considered as the ground truth.⁴⁵

2.3 | Hip arthroscopy (femoral osteochondroplasty)

A single fellowship-trained attending orthopedic surgeon, who specializes in hip arthroscopy, performed all operative procedures (S.J.N.). Cadaveric arthroscopic procedures were performed in the supine

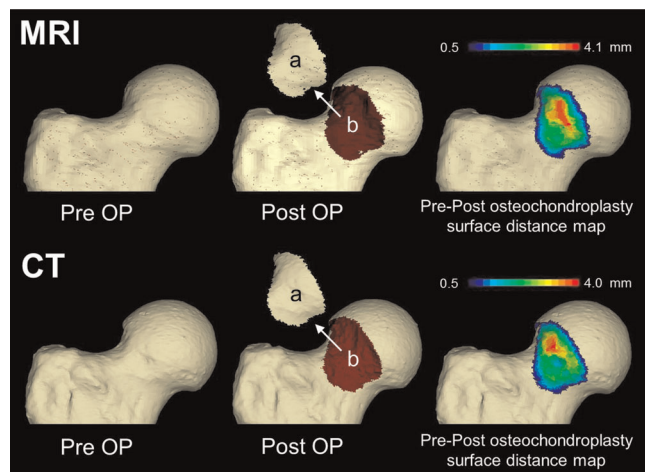


FIGURE 1 Comparison of 3D proximal femoral bone models of cadaveric specimens reconstructed from 1.5 T MRI and CT data. An image subtraction routine was used to quantify bone resected during femoral osteochondroplasty by computing the least-distance distribution (in mm) between preoperative (pre OP) and postoperative (post OP) models. a: Preosteochondroplasty surface model. b: Postosteochondroplasty surface model. CT, computed tomography; MRI, magnetic resonance imaging [Color figure can be viewed at wileyonlinelibrary.com]

position. Traction was applied to simulate standard intraoperative conditions. An anterolateral and modified mid anterior portal were established. An interportal capsulotomy was performed between the anterolateral and modified anterior portal to expose the acetabular rim. A distal accessory anterolateral (DALA) portal was then established. With the arthroscope in the anterior portal and an arthroscopic scalpel device in the DALA portal, a T-capsulotomy was then performed to allow visualization of the femoral neck. An arthroscopic femoral osteochondroplasty was performed from the lateral to medial synovial fold. Intraoperative fluoroscopy and direct arthroscopic visualization were used to evaluate the femoral head-neck junction. A femoral osteochondroplasty was performed to achieve a target postoperative alpha angle of 42° based on prior literature. Intraoperative fluoroscopy, as well as a dynamic hip examination throughout the osteochondroplasty, were performed to confirm complete removal of all abnormal bony morphology.

2.4 | Method for quantification of resected bone

The 3D bone surface models were compared by measuring the surface-to-surface least distance distribution between each pair of superimposed and aligned pre- and post-osteochondroplasty models. The accuracy of the alignment was less than 0.2° and 0.1 mm in two planes for rotations and translations, respectively.⁴⁶ 3D model registration and surface-to-surface least distance computation were performed with the same technique previously described.⁴⁶ Intra-rater reliability of the method had been previously tested giving a mean difference in the order of 10⁻² mm on test-retest (from

TABLE 1 Paired t-test of the 1.5 T MRI- and CT-based metrics used to quantify bone resected during femoral osteochondroplasty

	CT	MRI	p value
FSA (mm ²)	641.2 ± 184.8	615.8 ± 232.4	0.613
FV (mm ³)	950.6 ± 534.6	939.9 ± 536.6	0.919
FH _{mean} (mm)	1.7 ± 0.3	1.6 ± 0.4	0.555
FH _{max} (mm)	3.6 ± 0.6	3.7 ± 0.9	0.778

Abbreviations: CT, computed tomography; FSA, femoral osteochondroplasty surface area; FV, femoral osteochondroplasty volume; FH_{mean}, femoral osteochondroplasty mean height; FH_{max}, femoral osteochondroplasty maximum height; MRI, magnetic resonance imaging.

Supplementary Material from Malloy et al.).²⁵ The least distances over 0.5 mm at the headneck junction defined the region of bone resected during osteochondroplasty (Figure 1). Ultimately, the bone resected during the osteochondroplasty procedure was quantified using the following metrics: maximum and mean height in millimeters (mm), resected bone surface area (mm²) and resected bone volume (mm³).

2.5 | Statistical analysis

Shapiro-Wilk test was performed to determine the distribution of differences between imaging modalities for the metrics used to quantify the bony resection. The differences between imaging modalities for each metric were normally distributed. As such, paired sample t-tests were performed to compare the variables of interest as obtained from the MRI and CT bone models. The primary dependent variables of interest for this study were the metrics used to quantify the bone resected during femoral osteochondroplasty: maximum height (FH_{max}) (mm), mean height (FH_{mean}) (mm), surface area (mm²), and volume (FV) (mm³). All data are reported as means and standard deviations. An α value of 0.05 was chosen to determine statistical significance. One-tailed bivariate correlation analyses were performed with the hypothesis of a positive correlation between each MRI and CT based metric used to quantify bone resected during femoral osteochondroplasty. The strength of the bivariate correlations was defined as follows: weak (0.1–0.3), moderate (0.3–0.5), and strong as (0.5–1.00).⁴⁷ All statistical analyses were performed using SPSS (v. 26; IBM).

3 | RESULTS

3.1 | Comparison of MRI and CT based metrics

There were no differences between the MRI- and CT-based metrics used to quantify bone resected during femoral osteochondroplasty (Table 1 and Figure 2). The results indicate that the stability of the metrics is not dependent on the imaging modality used to create the

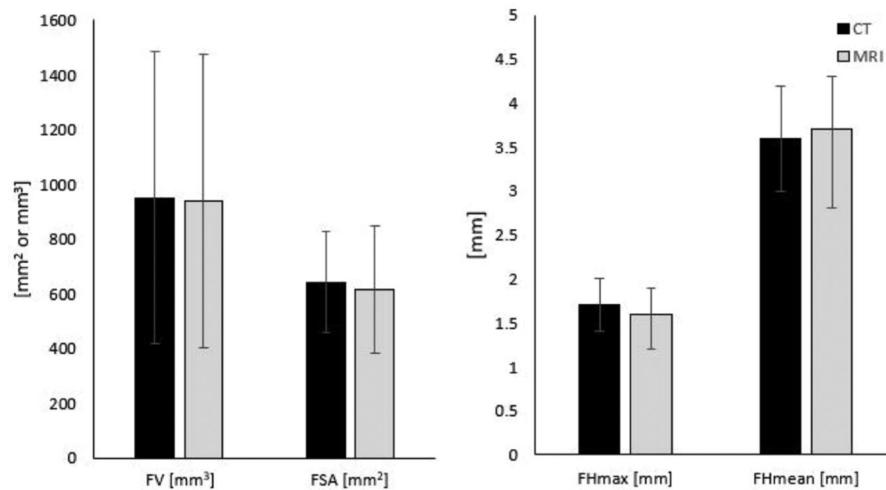


FIGURE 2 Barplots comparing average and standard deviations of the 1.5 T MRI- and CT-based metrics used to quantify bone resected during femoral osteochondroplasty. CT, computed tomography; FSA, femoral osteochondroplasty surface area; FV, femoral osteochondroplasty volume; FH_{mean}, femoral osteochondroplasty mean height; FH_{max}, femoral osteochondroplasty maximum height; MRI, magnetic resonance imaging

femoral surface model. This is also supported by the similar standard deviations obtained, as shown in Figure 2.

3.2 | Correlations between CT and MRI based metrics

There were strong bivariate correlations between MRI- and CT-based metrics for the quantification of bone resected during femoral osteochondroplasty (Table 2 and Figure 3).

4 | DISCUSSION

In this in vitro study, the amount of bone resected during hip arthroscopy was quantified using metrics generated from MRI and CT derived 3D models. The metrics were compared across imaging modalities that are currently used clinically to generate 3D bone models for surgical planning. The difference between the pre and postoperative 3D surface models generated from MRI and CT scans provided the metrics of bone resected volume, bone resected surface area, maximum resection height, and mean resection height. There were no differences between the metrics quantified on the different imaging modalities and the new metrics generated on each modality were strongly correlated. These findings indicate that the metrics to quantify the bony resection are stable across imaging modalities. This study provides new opportunities for advancing the quantification of proximal femur morphology by using 3D imaging methods that do not involve the risk associated with ionizing radiation exposure. This has important implications in the clinical setting as it can substantially help clinicians in assessing cam-type morphology in people with FAIS.

Prior studies have similarly reported MRI to provide accurate evaluation of cam-type morphology, as well as the 3D osseous anatomy of the proximal femoral neck.^{21,23–25,29–32} When compared to 3D models reconstruction derived from CT scan, Samim and colleagues²³ reported equivalent inter-rater agreement for the diagnosis of the presence and location of cam-type morphology in

TABLE 2 One-tailed bivariate correlation of 1.5 T MRI- and CT-based metrics used to quantify bone resected during femoral osteochondroplasty

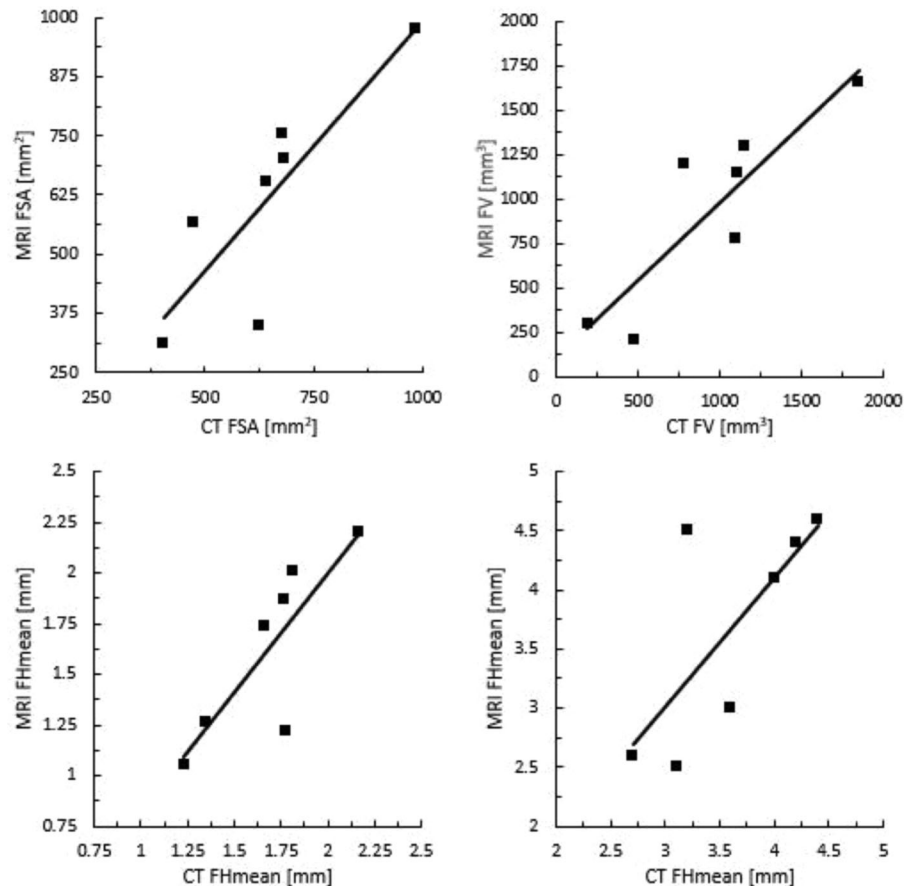
	<i>r</i>	<i>p</i> value
FSA (mm ²)	0.842	0.009 ^a
FV (mm ³)	0.878	0.005 ^a
FH _{mean} (mm)	0.830	0.010 ^a
FH _{max} (mm)	0.728	0.032 ^a

Note: All other variables were analyzed by Pearson correlation analysis. Abbreviations: CT, computed tomography; FSA, femoral osteochondroplasty surface area; FV, femoral osteochondroplasty volume; FH_{mean}, femoral osteochondroplasty mean height; FH_{max}, femoral osteochondroplasty maximum height; MRI, magnetic resonance imaging. ^aIndicates statistical significance at 0.05.

17 patients (*n* = 19 hips) using 3D models generated from 3 T MRI. The authors also noted that MRI effectively spared each patient an average radiation effective dose of 3.09 mSv for a total reduction of 479 mSv over the course of 4 years. Indeed, a radiological hip examination and a CT examination of the pelvis subject the patient to an average effective dose of 0.7 and 6 mSv, respectively, where an annual effective dose between 3 and 20 mSv is already considered as moderate and the threshold effective dose estimate for deterministic effects is 5 mSv.^{48–50} Meanwhile, utilizing four bilateral cadaveric pelvic specimens undergoing CT, MRI and laser scanning, Malloy and colleagues reported 1.5 T MRI to produce 3D femoral surface models more closely representing the actual bony surface anatomy when compared to CT derived models.²⁵ These results suggest that 3D MRI may be utilized as an alternative to 3D CT for the quantification of cam-type FAIS bony deformities corrected with a femoral osteochondroplasty procedure, while limiting radiation exposure.

The current clinical management for people undergoing hip arthroscopy for FAIS typically involves sets of pre and postoperative radiographs to quantify femoral morphology. In some cases of more severe deformity, CT imaging is used to generate 3D models to further assess 3D morphology for surgical planning, and in cases of revision hip

FIGURE 3 Scatterplots showing correlation between MRI- and CT-based metrics used to quantify bone resected during femoral osteochondroplasty. CT, computed tomography; FSA, femoral osteochondroplasty surface area; FV, femoral osteochondroplasty volume; FH_{mean} , femoral osteochondroplasty mean height; FH_{max} , femoral osteochondroplasty maximum height; MRI, magnetic resonance imaging



arthroscopy more scans requiring ionizing radiation exposure may be required. Residual camdeformity, a consequence of incomplete cam resection, has been shown to be the most commonly encountered condition in patients undergoing revision hip arthroscopy.^{17–19} In their retrospective study of patients ($n = 47$ patients; $n = 50$ hips) undergoing revision hip arthroscopy, Ross and colleagues reported residual cam deformity to be the most common reason for revision surgery.¹⁶ Residual cam deformities were most frequently encountered at the superolateral headneck junction, with a mean elevated alpha angle ($>68 \pm 16^\circ$) between the 12:00 and 2:30 positions, likely reflecting the challenge of the surgeon in accessing this portion of the femoral head. It has been shown that novice surgeons performing hip arthroscopy require a considerable amount of procedures to become proficient.^{51–53} Providing a volumetric characterization and preoperative visualization of the extent and location of cam deformity by using methods based on 3D reconstructed models is fundamental to minimize the prevalence of revision arthroscopy due to inadequate preoperative planning and consequent bony structural correction. It is also imperative that these measures can be obtained using imaging that does not involve the risk of unnecessary ionizing radiation exposure.

4.1 | Limitations

This in vitro experimental study was not without limitations. The sample size in the current in vitro study was small making the

findings at risk for Type II statistical error due to being underpowered. However, the sample size used in the current study was consistent with similar types of in vitro cadaveric investigations.^{30,54–57} Additionally, the parametric tests used in this study have been shown to be applicable in studies with extremely small sample sizes, defined as 5 or less.⁵⁸ While radiography is part of the standard workup in symptomatic patients with FAIS, CT, and MRI yield the additional metrics of cam resection analyzed in this investigation which are not measurable using 2D imaging. Not all of the considered specimens were found to possess a true cam deformity, based on the alpha angle measured on axial slices. Nevertheless, only very recently was a threshold of 60° recommended to define cam morphology as a pathologic deformity on radiographs.⁵⁹ In hindsight, it is not feasible to include cam lesions as desirable features for the cadaver specimens. However, utilization of cadaveric specimens was essential to allow for comparison of MRI and CT based metrics to quantify bone resected during femoral osteochondroplasty, as the performance of CT postoperatively on patients is not standard practice due to radiation exposure. Variability in the size of the femoral head was present, potentially confounding our measurements. The larger variability in the size could be due to the small sample size ($n = 7$). However, as we included small cam deformities in this study, we were prone to higher errors, therefore the application of the technique to femurs with known larger cam deformity would potentially give better results. Additionally, the femoral head size was not a fundamental parameter to control for the

purpose of this preliminary investigation. It will be important to consider a normalization for the femoral head size for future studies involving the measurement of alpha angles or the development of new measures in the context of FAIS. Nonetheless, prior studies have reported differences in femoral head volumes, with significantly larger heads in males when compared to females, with increasing head size being positively correlated with increasing patient height.^{8,14} Further studies should seek to normalize cam-type morphology related measurements before and following femoral osteochondroplasty based on femoral head size.

5 | CONCLUSION

Pre and postoperative MRI and CT derived 3D bone models can be used to quantify the amount of bone resected during femoral osteochondroplasty, without significant differences between the imaging modalities.

ACKNOWLEDGMENTS

The authors are thankful for funding from the Aircast Foundation and Michael and Jacqueline Newman. Stryker Corporation is acknowledged for donating the cadaveric specimens.

CONFLICT OF INTERESTS

The authors did not identify any conflict of interest and disclose the following collaborations: Martina Guidetti (none), Philip Malloy (none), Thomas D. Alter (none), Alexander C. Newhouse (none), Alejandro A. Espinoza Orías (PLOS One: Editorial/governing board, Stryker: Other financial or material support), Nozomu Inoue (National Institutes of Health: Research Support), Shane J. Nho (Allosource: Research support, American Orthopaedic Association: Board or committee member, American Orthopaedic Society for Sports Medicine: Board or committee member, Arthrex, Inc: Research support, Arthroscopy of North America: Board or committee member, Athletico: Research support, DJ Orthopaedics: Research support, Linvatec: Research support, Miomed: Research support, Ossur: IP royalties, Smith & Nephew: Research support, Springer: Publishing royalties, financial or material support, Stryker: IP royalties; Paid consultant; Research support).

AUTHORS CONTRIBUTIONS

Thomas D. Alter, Martina Guidetti, Alexander C. Newhouse, Alejandro A. Espinoza Orías, Philip Malloy, Nozomu Inoue, and Shane J. Nho completed data analysis. Thomas D. Alter, Martina Guidetti, Alexander C. Newhouse, and Nozomu Inoue completed interpretation of the data. All authors completed drafting/revising the paper. Thomas D. Alter, Martina Guidetti, Alexander C. Newhouse, Philip Malloy, and Alejandro A. Espinoza Orías completed critical review of the final manuscript.

ORCID

Martina Guidetti  <http://orcid.org/0000-0001-8882-4386>

Philip Malloy  <http://orcid.org/0000-0003-2543-3198>

Alejandro A. Espinoza Orías  <http://orcid.org/0000-0002-3792-515X>

Shane J. Nho  <http://orcid.org/0000-0003-2126-2766>

REFERENCES

1. Clohisy JC, Zebala LP, Nepple JJ, Pashos G. Combined hip arthroscopy and limited open osteochondroplasty for anterior femoroacetabular impingement. *J Bone Joint Surg.* 2010;92:1697-1706.
2. Bonazza NA, Homcha B, Liu G, Leslie DL, Dhawan A. Surgical trends in arthroscopic hip surgery using a large national database. *Arthroscopy.* 2018;34:1825-1830.
3. Freeman CR, Azzam MG, Leunig M. Hip preservation surgery: surgical care for femoroacetabular impingement and the possibility of preventing hip osteoarthritis. *J Hip Preserv Surg.* 2014;1:46-55.
4. Van Houcke J, Khanduja V, Audenaert EA. Accurate arthroscopic cam resection normalizes contact stresses in patients with femoroacetabular impingement. *Am J Sports Med.* 2021;49:42-48.
5. Wong TT, Lynch TS, Popkin CA, Kazam JK. Preoperative use of a 3D printed model for femoroacetabular impingement surgery and its effect on planned osteoplasty. *Am J Roentgenol.* 2018;211:W116-W121.
6. Audenaert E, Smet B, Pattyn C, Khanduja V. Imageless versus imagebased registration in navigated arthroscopy of the hip: A cadaverbased assessment. *J Bone Joint Surg Br.* 2012;94:624-629.
7. Van Houcke J, Khanduja V, Sueys L, et al. Accuracy of navigated cam resection in femoroacetabular impingement: A randomized controlled trial. *J Hip Preserv Surg.* 2016;3:3.
8. Zhang L, Wells JE, Dessouky R, et al. 3D CT segmentation of Cam type femoroacetabular impingement—reliability and relationship of Cam lesion with anthropomorphic features. *Br J Radiol.* 2018;91:20180371.
9. Tannast M, Kubiak-Langer M, Langlotz F, Puls M, Murphy SB, Siebenrock KA. Noninvasive three-dimensional assessment of femoroacetabular impingement. *J Orthop Res.* 2007;25:122-131.
10. Bouma H, Hogervorst T, Audenaert E, van Kampen P. Combining femoral and acetabular parameters in femoroacetabular impingement: the omega surface. *Med Biol Eng Comput.* 2015;53:1239-1246.
11. Griffin DR, Dickenson EJ, O'donnell J, et al. The Warwick agreement on femoroacetabular impingement syndrome (FAI syndrome): an international consensus statement. *Br J Sports Med.* 2016;50:1169-1176.
12. Larson CM. Editorial Commentary: "The Earth is Not Flat": Progressing from plain radiographs to three dimensional imaging when evaluating hip disorders. 2020:2633-2634.
13. Taghizadeh E, Chandran V, Reyes M, Zysset P, Buehler P. Statistical analysis of the interindividual variations of the bone shape, volume fraction and fabric and their correlations in the proximal femur. *Bone.* 2017;103:252-261.
14. Yanke AB, Khair MM, Stanley R, et al. Sex differences in patients with CAM deformities with femoroacetabular impingement: 3 dimensional computed tomographic quantification. *Arthroscopy.* 2015;31:2301-2306.
15. Keating TC, Leong N, Beck EC, et al. Evaluation of statistical shape modeling in quantifying femoral morphologic differences between symptomatic and nonsymptomatic hips in patients with unilateral femoroacetabular impingement syndrome. *Arthrosc Sports Med Rehabil.* 2020;2:e91-e95.
16. Ross JR, Larson CM, Adeoye O, Kelly BT, Bedi A. Residual deformity is the most common reason for revision hip arthroscopy: a three dimensional CT study. *Clin Orthop Relat Res.* 2015;473:1388-1395.
17. Clohisy JC, St John LC, Schutz AL. Surgical treatment of femoroacetabular impingement: a systematic review of the literature. *Clin Orthop Relat Res.* 2010;468:555-564.

18. Bogunovic L, Gottlieb M, Pashos G, Baca G, Clohisey JC. Why do hip arthroscopy procedures fail? *Clin Orthop Relat Res.* 2013;471:2523-2529.
19. Heyworth BE, Shindle MK, Voos JE, Rudzki JR, Kelly BT. Radiologic and intraoperative findings in revision hip arthroscopy. *Arthroscopy.* 2007;23:1295-1302.
20. Degen RM, Mayer SW, Fields KG, Coleman SH, Kelly BT, Nawabi DH. Functional outcomes and cam recurrence after arthroscopic treatment of femoroacetabular impingement in adolescents. *Arthroscopy.* 2017;33:1361-1369.
21. Lerch TD, Degonda C, Schmaranzer F, et al. Patientspecific 3d magnetic resonance imaging-based dynamic simulation of hip impingement and range of motion can replace 3d computed tomography-based simulation for patients with femoroacetabular impingement: implications for planning open hip preservation surgery and hip arthroscopy. *Am J Sports Med.* 2019;47:2966-2977.
22. Ito K, Minka MA II, Leunig M, Werlen S, Ganz R. Femoroacetabular impingement and the cam effect: a MRIbased quantitative anatomical study of the femoral headneck offset. *J Bone Joint Surg Br.* 2001;83:171-176.
23. Samim M, Eftekhary N, Vigdorich JM, et al. 3DMRI versus 3DCT in the evaluation of osseous anatomy in femoroacetabular impingement using Dixon 3D FLASH sequence. *Skeletal Radiol.* 2019;48:429-436.
24. Radetzki F, Saul B, Hagel A, et al. Threedimensional virtual simulation and evaluation of the femoroacetabular impingement based on "black bone" MRA. *Arch Orthop Trauma Surg.* 2015;135:667-671.
25. Malloy P, Gasienica J, Dawe R, et al. 1.5 T magnetic resonance imaging generates accurate 3D proximal femoral models: surgical planning implications for femoroacetabular impingement. *J Orthop Res.* 2020;38:2050-2056.
26. Lee C, Jeon KJ, Han SS, et al. CTlike MRI using the zeroTE technique for osseous changes of the TMJ. *Dentomaxillofacial Radiol.* 2020;49:20190272.
27. Koh E, Walton ER, Watson P. VIBE MRI: an alternative to CT in the imaging of sportsrelated osseous pathology? *Br J Radiol.* 2018;91:20170815.
28. Breighner RE, Bogner EA, Lee SC, Koff MF, Potter HG. Evaluation of osseous morphology of the hip using zero echo time magnetic resonance imaging. *Am J Sports Med.* 2019;47:3460-3468.
29. Gyftopoulos S, Yemin A, Mulholland T, et al. 3DMR osseous reconstructions of the shoulder using a gradientecho based twopoint Dixon reconstruction: a feasibility study. *Skeletal Radiol.* 2013;42:347-352.
30. Neubert A, Wilson KJ, Engstrom C, et al. Comparison of 3D bone models of the knee joint derived from CT and 3 T MR imaging. *Eur J Radiol.* 2017;93:178-184.
31. Liang X, Jacobs R, Hassan B, et al. A comparative evaluation of cone beam computed tomography (CBCT) and multislice CT (MSCT): Part i. on subjective image quality. *Eur J Radiol.* 2010;75:265-269.
32. Rathnayaka K, Momot KI, Noser H, et al. Quantification of the accuracy of MRI generated 3D models of long bones compared to CT generated 3D models. *Med Eng Phys.* 2012;34:357-363.
33. Lansdown DA, Cvetanovich GL, Verma NN, et al. Automated 3-dimensional magnetic resonance imaging allows for accurate evaluation of glenoid bone loss compared with 3-dimensional computed tomography. *Arthroscopy.* 2019;35:734-740.
34. Mallow GM, Siyaji ZK, Galbusera F, et al. Intelligence-based spine care model: a new era of research and clinical decision making. 2021:135-145.
35. Jolly MP, Alvino C, Odry B, et al. Automatic femur segmentation and condyle line detection in 3D MR scans for alignment of high resolution MR. 2010 IEEE International Symposium on Biomedical Imaging: From Nano to Macro. IEEE, 2010;940-943.
36. Deniz CM, Xiang S, Hallyburton RS, et al. Segmentation of the proximal femur from MR images using deep convolutional neural networks. *Sci Rep.* 2018;8:1-14.
37. Arezoomand S, Lee WS, Rakhra KS, Beaulé PE. A 3D active model framework for segmentation of proximal femur in MR images. *Int J Comput Assist Radiol Surg.* 2015;10:55-66.
38. Zeng G, Schmaranzer F, Degonda C, et al. MRIbased 3D models of the hip joint enables radiationfree computerassisted planning of periacetabular osteotomy for treatment of hip dysplasia using deep learning for automatic segmentation. *Eur J Radiol Open.* 2021;8:100303.
39. Zeng G, Yang X, Li J, et al. 3D Unet with multilevel deep supervision: Fully automatic segmentation of proximal femur in 3D MR images. *International Workshop on Machine Learning in Medical Imaging.* Springer; 2017:274-282.
40. Zeng G, Wang Q, Lerch T, et al. Latent 3D Unet: Multilevel latent shape space constrained 3D Unet for automatic segmentation of the proximal femur from radial MRI of the hip. *International Workshop on Machine Learning in Medical Imaging.* Springer; 2018:188-196.
41. Huang ZG, Zhang XZ, Hong W, et al. The application of MR imaging in the detection of hip involvement in patients with ankylosing spondylitis. *Eur J Radiol.* 2013;82:1487-1493.
42. Tresch F, Dietrich TJ, Pfirrmann CW, Sutter R. Hip MRI: Prevalence of articular cartilage defects and labral tears in asymptomatic volunteers. a comparison with a matched population of patients with femoroacetabular impingement. *J Magn Reson Imaging.* 2017;46:440-451.
43. Poon S, Chen YH, Wendolowski SF, et al. Cadaveric study of the safety and device functionality of magnetically controlled growing rods after exposure to magnetic resonance imaging. *Spine Deform.* 2018;6:290-298.
44. Dirim B, Haghighi P, Trudell D, Portes G, Resnick D. Medial patellofemoral ligament: Cadaveric investigation of anatomy with MRI, MR arthrography, and histologic correlation. *Am J Roentgenol.* 2008;191:490-498.
45. Van den Broeck J, Vereecke E, Wirix Speetjens R, Vander Sloten J. Segmentation accuracy of long bones. *Med Eng Phys.* 2014;36:949-953.
46. Ochia RS, Inoue N, Renner SM, et al. Threedimensional in vivo measurement of lumbar spine segmental motion. *Spine (Phila Pa 1976).* 2006;31:2073-2078.
47. Cohen J. Statistical power analysis for the behavioural sciences. 2013.
48. Mettler, Jr., FA, Huda W, Yoshizumi TT, Mahesh M. Effective doses in radiology and diagnostic nuclear medicine: a catalog. *Radiology.* 2008;248:254-263.
49. Fazel R, Krumholz HM, Wang Y, et al. Exposure to lowdose ionizing radiation from medical imaging procedures. *N Engl J Med.* 2009;361:849-857.
50. Thome C, Chambers DB, Hooker AM, Thompson JW, Boreham DR. Deterministic effects to the lens of the eye following ionizing radiation exposure: is there evidence to support a reduction in threshold dose? *Health Phys.* 2018;114:328-343.
51. Mehta N, Chamberlin P, Marx RG, et al. Defining the learning curve for hip arthroscopy: a threshold analysis of the volumeoutcomes relationship. *Am J Sports Med.* 2018;46:1284-1293.
52. Hoppe DJ, de Sa D, Simunovic N, et al. The learning curve for hip arthroscopy: a systematic review. *Arthroscopy.* 2014;30:389-397.
53. Go CC, Kyin C, Maldonado DR, Domb BG. Surgeon experience in hip arthroscopy affects surgical time, complication rate, and reoperation rate: a systematic review on the learning curve. *Arthroscopy: The Journal of Arthroscopic & Related Surgery.* 2020;36:3092-3105.
54. Yanke AB, Shin JJ, Pearson I, et al. Threedimensional magnetic resonance imaging quantification of glenoid bone loss is equivalent to 3dimensional computed tomography quantification: Cadaveric study. *Arthroscopy.* 2017;33:709-715.
55. Lockard CA, Stake IK, Brady AW, et al. Accuracy of MRIbased talar cartilage thickness measurement and talus bone and cartilage

- modeling: comparison with ground truth laser scan measurements. *Cartilage*. 2020;1947603520976774.
56. Suppauksorn S, Beck EC, Rasio J, et al. A cadaveric study of camtype femoroac etabular impingement: Biomechanical comparison of contact pressures between cam morphology, partial femoral osteoplasty, and complete femoral osteoplasty. *Arthroscopy*. 2020;36:2425-2432.
57. Logishetty K, Van Arkel RJ, Ng K, Muirhead-Allwood SK, Cobb JP, Jeffers J. Hip capsule biomechanics after arthroplasty: the effect of implant, approach, and surgical repair. *Bone Joint J*. 2019;101:426-434.
58. De WJC. Using the Student's *t* test with extremely small sample sizes. *Pract Assess Res Eval*. 2013;18:10.
59. van Klij P, Reiman MP, Waarsing JH, et al. Classifying cam morphology by the alpha angle: a systematic review on threshold values. *Orthop J Sports Med*. 2020;8:2325967120938312.

How to cite this article: Guidetti M, Malloy P, Alter TD, et al. MRI and CT-based metrics for the quantification of arthroscopic bone resections in femoroacetabular impingement syndrome. *J Orthop Res*. 2021;1-8.
<https://doi.org/10.1002/jor.25139>